ESI Preprints **Not Peer-reviewed**

Energy Valorization of Marine Algae of the Type *Ulva sp.* Through the Manufacture of Combustible Briquettes

Kalidou Ba
Mamadou Faye
Alpha Ousmane Toure
Water, Energy, Environment and Industrial Processes Laboratory (LE3PI),
Ecole Supérieure Polytechnique (ESP), Dakar-Fann, Senegal
Cheikh Anta DIOP University of Dakar, Dakar-Fann, Senegal

Approved: 13 April 2026
Posted: 15 April 2026

Cite As:
Ba, K., Faye, M. & Toure, A.O. (2026). *Energy Valorization of Marine Algae of the Type Ulva sp. Through the Manufacture of Combustible Briquettes*. ESI Preprints.
https://doi.org/10.19044/esipreprint.4.2026.p452

Abstract

Algae briquettes today represent a major international challenge in terms of reducing greenhouse gases and the energy transition. They offer a sustainable and renewable alternative to global dependence on fossil fuels. This study aims to valorize macroalgae of the genus *Ulva sp.*, recovered from the pier of the C3 power plant of SENELEC in Dakar, Senegal, into combustible briquettes intended to play a similar role as charcoal and butane gas for cooking. The production method consists of mixing a constant mass of algae powder with a varying percentage (20% to 50%) of a mineral binder obtained from fluosilicic acid, a waste product from Senegalese chemical industries. The formulation yielded four briquette models: BAL50, BAL40, BAL30, and BAL20. Physicochemical analyses as well as combustion evaluations were carried out to assess the quality of the combustible briquettes. The results obtained showed that BAL20 have a lower heating value (LHV) of 2254 Kcal/Kg and a consumption time of 85 min, superior to BAL50, BAL40, and BAL30. Analysis of variance showed that the effect of ash content is highly significant ($p = 0.0307 < 5\%$), indicating a clear influence of ash content on LHV.

Keywords: Briquette, fuel, algae, valorization

1. Introduction

The use of current energy sources such as fossil fuels poses a real environmental problem, particularly concerning air and water pollution in recent years (François et al., 2025; Sundaram et al., 2025). These negative consequences have sparked interest in developing new technologies to obtain clean energy, mainly through the valorization of surplus plant and animal residues (Nzihou et al., 2024; Rath et al., 2024). According to recent statistics from the Food and Agriculture Organization (FAO), world marine algae production has continued to increase. Approximately 30.1 million tonnes of aquatic plants (mainly seaweeds, worth 11.7 billion US dollars) were produced in 2016, more than double the value recorded in 2000 (FAO, 2024). Marine algae are considered an important biomass source for energy production due to their rapid growth and photosynthetic efficiency; however, their use in energy valorization remains limited globally (Baghel et al., 2020; Yaman & Kucukbayrak, 2013). Current uses of aquatic biomass mainly involve the production of cosmetics, fertilizers, industrial gums (phycocolloids), chemicals, and food, particularly in Asia (Jabeen et al., 2025; C. Li et al., 2024). Several researchers have studied the technical feasibility of transforming marine microalgae into a renewable energy source. For example, van Hal et al. proposed the synthesis of butanol and biogas from microalgae by fermentation and anaerobic digestion, respectively (Wal et al., 2013). Other researchers such as Kim et al. worked on the co-production of alginate and biodiesel from a brown seaweed called *Laminaria japonica*, through the heterotrophic culture of an oleaginous yeast in the supernatant liquid of the autoclaved algae solution before solid-phase alginate extraction (Kim et al., 2019; Yaman & Kucukbayrak, 2013). Among the macroalgae present in Senegal are green algae of the genus *Ulva sp.*, which are considered one of the most promising biomass sources (Amrullah et al., 2022). They are relatively poor in carbon but often rich in nitrogen, phosphorus, and other nutrients compared to many types of terrestrial biomass (Bird et al., 2011). At the cooling water intake of the condensers at the Cap des Biches power plant in Dakar, 3,852,000 kg of fresh *Ulva sp.* are recovered per season (March to August). This is a potentially energetic biomass facing a valorization problem. Their presence is partly due to the discharge of untreated waste or wastewater into the sea, which causes their proliferation. Once collected, exposure to the sun accelerates the putrefaction process, producing hydrogen sulfide, ammonia, and methane (Ahmed et al., 2024). At certain concentrations, these gases can be very dangerous for humans and animals (Britt et al., 2004; Jo et al., 2013; Lars Ole et al., 2023). In this context, we propose to valorize algal biomass in the form of combustible briquettes, an alternative to conventional coal that could be used in households as well as on an industrial scale.

2. Materials and Methods

2.1. Raw Material

A mass of 50 kg of *Ulva sp.* is collected at the pier after being retained by the BAUDREY filters. It is then transported to the laboratory to be dried out of the sun at room temperature for at least 24 hours, spread on a flat surface for better aeration. This step is important for determining the moisture content of the fresh algae. The second step consists of drying the algae in an oven at a temperature of about 60°C for 24 hours. After this step, they are ground using a metal pestle and mortar, then sieved with a 300 µm mesh sieve. The *Ulva* used are shown in Figure 1.

Figure 1: *Ulva sp.*, near the "Cap des Biches" channel

2.2. Binder Synthesis (Calcium Silicate)

Under normal temperature and pressure conditions, a volume of 377 mL of 25% fluosilicic acid reacts instantly with a mass of 90 g of sodium chloride (NaCl). According to stoichiometric proportions, this reaction produces hydrochloric acid (18% HCl) and sodium fluorosilicate (Na_2SiF_6), which precipitates as a thick gelatinous cake. The time required for this reaction is 15 minutes. At the end of this reaction, vacuum filtration was carried out. The hydrochloric acid obtained is collected in a vacuum flask, and the sodium fluorosilicate is retained on the filter as a cake. This precipitate is then dried at 110 °C in a MEMMERT-type oven for 24 hours. The simplified process of this first synthesis step is illustrated in Figure 2.

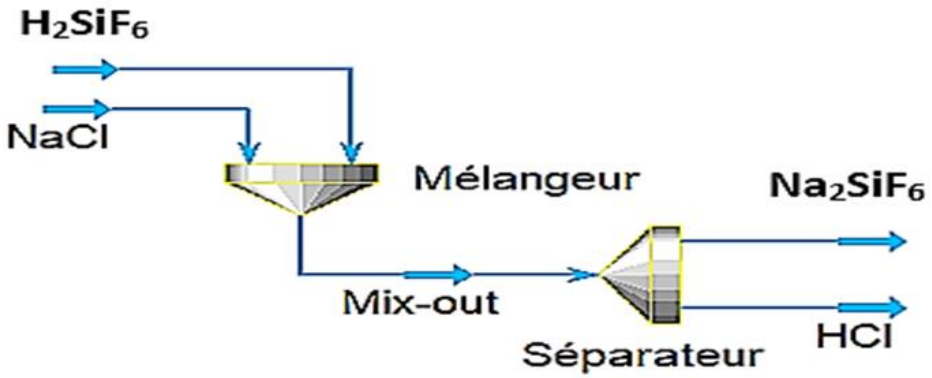

Figure 2: Process for obtaining sodium fluorosilicate

The sodium fluorosilicate (Na_2SiF_6) obtained in the first synthesis step, after being filtered, dried, and ground, is causticized with slaked lime for 150 minutes at 50°C. This process first involves mixing 100 g of sodium fluorosilicate with 600 mL of distilled water heated to 50°C. Then, 114.15 g of slaked lime is added. At the end of the process, vacuum filtration is performed to recover the aqueous phase, which constitutes the sodium silicate. A simplified diagram of the process is shown in Figure 3.

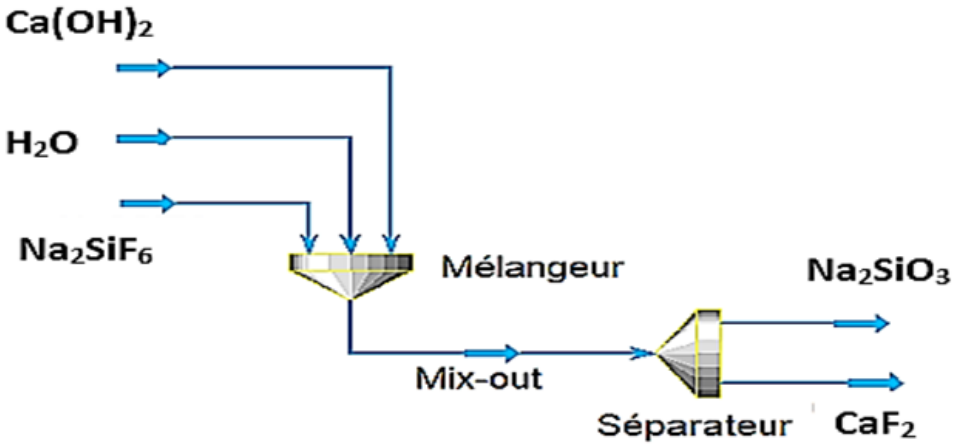

Figure 3: Process for obtaining sodium silicate

The sodium silicate thus obtained is subjected to a new caustification with 43.29 g of $Ca(OH)_2$ at a temperature of 50°C for 150 minutes to obtain calcium silicate and a 3% sodium hydroxide solution (BA et al., 2022). Vacuum filtration is carried out to separate the solid and aqueous phases. The obtained cake is dried in an oven, and the yield of calcium silicate obtained is 78.67%. This process is illustrated in Figure 4.

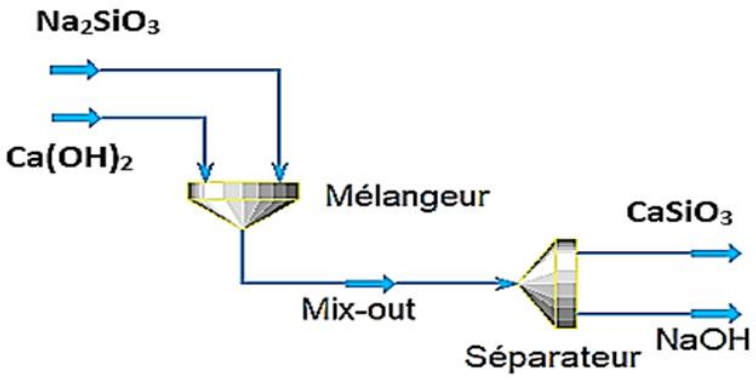

Figure 4: Process for obtaining calcium silicate

2.3. Briquette Production Method

The extruder used for briquette compression is of artisanal design. It consists of a three-phase 0.075 kW motor and has a mass of 16.29 kg. Inside the cylinder, there is a screw rotating at a speed of 280 rpm which compresses the paste (Figure 5). After compression, the combustible briquettes emerge in a cylindrical shape thanks to a cone placed at the extruder outlet. The production capacity of this machine is about 200 kg/h. To study the effect of binder content with a total mass of 500g, five types of briquettes were produced by varying the binder percentage from 20 to 50%, namely BAL50 (Briquettes with 50% $CaSiO_3$), BAL40 (Briquettes with 40% $CaSiO_3$), BAL30 (Briquettes with 30% $CaSiO_3$), and BAL20 (Briquettes with 20% $CaSiO_3$). However, a constant quantity of wood chips (about 20%) was added to each sample to increase the density of the mixture and improve its malleability since the algae powder alone is very light. The process diagram is shown in Figure 6.

Figure 5: EMIE type extruder

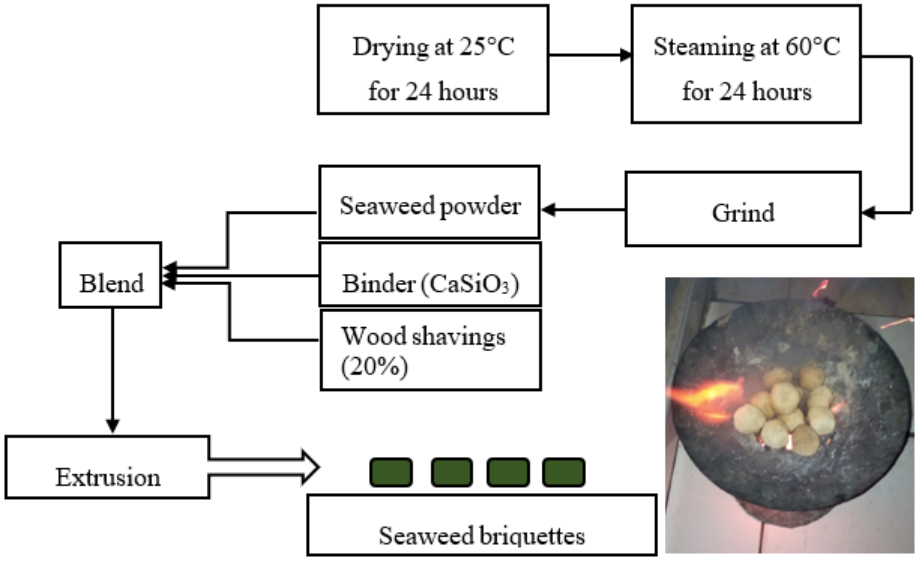

Figure 6: Production process for Ulva sp.-based briquettes

2.4. Characterization of Combustible Briquettes

2.4.1. Physical and chemical Analyses

After the formulation step, the combustible briquettes are characterized by determining moisture, ash content, and lower heating value. These analyses were carried out by the DANGOTE Cement analysis laboratory using the NF B55-101 standard.

2.4.1.1. X-Ray Fluorescence (XRF) Analysis

The mineral composition was determined by X-ray fluorescence spectrometry, using a Niton XL3T XRF analyzer connected to a computer equipped with NDTr 6.5.2 software for data acquisition and processing. This is a rapid, non-destructive, multi-element analysis technique allowing the identification and quantification of most chemical elements present in a sample.

For each analysis, an amount of 1.2 g of powder was mixed with 0.12 g of binder (Hoescht wax), then introduced into a compression die. A pressure of about 15 tonnes was applied using a press for 2 to 3 minutes to obtain a compact pellet suitable for analysis. The pellets were then analyzed using the Niton XL3T XRF analyzer, previously calibrated using certified standards.

2.4.1.2. Determination of Moisture Content

To determine the moisture content (H), 2 g of each briquette sample were weighed into a crucible of known mass. The crucible containing the sample was placed in an oven at 105°C. The crucible was removed and

placed in a desiccator, allowed to cool to room temperature, and then reweighed. This operation was repeated until a constant mass was obtained. It is calculated using Equation 1.

$$H = \frac{m_1 - m_2}{m_2} * 100 \quad (1)$$

With:
m_1: initial mass of the sample (g)
m_2: final mass of the dried sample (g)

2.4.1.3. Ash Content

Ash content (AC) was determined by weighing 2 grams of oven-dried briquettes into a crucible of known mass. The briquette was placed in a furnace for about 3 hours and maintained at a constant temperature of 600 °C until ash was obtained. Ash content was calculated using Equation 2.

$$AC = \frac{m_4}{m_3} * 100 \quad (2)$$

m_3: mass of the dried sample (g)
m_4: mass of ash (g)

2.4.1.4. Total Organic Carbon Content

Total organic carbon (TOC) was determined by the Walkley-Black method, based on oxidation by potassium dichromate in an acidic medium, followed by titration with ferrous sulfate. The samples were ground, and a mass between 0.1 g and 1 g was introduced into an Erlenmeyer flask. This test portion was mixed with 10 mL of 1 N potassium dichromate solution and 20 mL of concentrated sulfuric acid. The mixture was shaken for 1 minute and then left to stand for 30 minutes. Then, 200 mL of distilled water, 10 mL of phosphoric acid, and 10 to 15 drops of ferroin indicator solution were added. The resulting solution was titrated with 0.5 N ferrous sulfate. The percentage of carbon in the sample is determined using Equation 3.

$$TOC = \frac{(A - B) * V * G * 100}{P * A} \quad (3)$$

With V=10 mL and G=0.004
C: organic carbon concentration (%)
A: volume of ferrous sulfate used for the blank (mL)
B: volume of ferrous sulfate used for the sample (mL)
V: initial volume of dichromate added
G: number of g of C per mL of dichromate
P: weight of the titrated sample expressed on a dry basis (g)

2.4.1.4. Determination of Gross Calorific Value

The calorific value was determined using an XRY-1A type calorimetric bomb. The procedure involves placing the sample on the sample holder in the bomb. The ignition wire is connected to the support and the ignition circuit, and then the bomb is sealed. Several purge cycles are carried out, followed by filling the bomb with O_2 at the specified pressure (20-30 bar), checking for leaks. The bomb is then immersed in the calorimeter, which is filled with a known mass of water, and the stirring system is started. When the initial temperature (T_i) becomes stable, it's recorded, and electrical ignition is triggered to achieve complete combustion. After combustion, the final temperature (T_f) of the system in its stable state is recorded. The temperature change (ΔT), the net energy released by combustion (Q_{total}), the corrected net energy released (Q_{sample}), the gross calorific value (GCV), and the net calorific value (NCV) are calculated using the following equations:

$$\Delta T = T_f - T_i \quad (4)$$

$$Q_{total} = K\Delta T \quad (5)$$

$$Q_{sample} = Q_{total} - Q_{wire} - Q_{other\ corrections} \quad (6)$$

$$PCS = \frac{Q_{sample}}{m} \quad (7)$$

$$PCI = PCS - \left(m_{H2O} - \Delta H_{vap}\right) \quad (8)$$

With:

K: Calorimetric constant of the system (J/°C), obtained by calibration

Q_{wire}: energy supplied by the ignition wire, determined by test or provided

$Q_{other\ corrections}$: includes small thermochemical corrections related to secondary reactions occurring in the bomb

m: mass of the sample (g)

m_{H2O}: mass of water formed during combustion, per kg of fuel

ΔH_{vap}: latent heat of vaporization of water

2.4.2. Mechanical Test

This involves determining the shatter resistance (RC), to evaluate the behavior of briquettes during handling, transport, and unloading. The method follows the ASTM D440-49 standard. It consists of dropping a briquette three times onto a solid surface from a height of 1.8 m. The mass of the briquette is measured before the test. Shatter resistance is then calculated using Equation 9 (Lomunyak et al., 2024).

$$RC = 100 - \frac{m_0 - m_1}{m_0} * 100 \quad (9)$$

m_0: is the mass of the briquette obtained before the drop
m_1: is the mass of the briquette after tumbling

2.4.3. Combustion Test

This analysis determines the thermal characteristics of the briquettes, notably the water boiling time, ignition time, and consumption time. For this, a coffee maker containing 250 mL of water is heated on a stove fueled by 250 g of briquettes, in the absence of an air draft to simulate normal cooking conditions. The water temperature is recorded every 5 minutes using a probe thermometer.

2.4.4. Analysis of Variance (ANOVA)

To evaluate the influence of ash content (ASH), total organic carbon (TOC), and moisture (H) on the lower heating value (LHV) of the briquettes, an analysis of variance (ANOVA) was performed. It allows comparing the variability explained by each factor against the residual variability of the model. ANOVA tests the null hypothesis (H_0) that all coefficients associated with each variable are zero, meaning that none of the considered parameters have a significant effect on LHV. The alternative hypothesis (H_1) states that at least one factor exerts an influence on LHV.

3. Results and Discussion

3.1. Characterization of *Ulva* by X-Ray Fluorescence (XRF)

The different values obtained during characterization are recorded in Table I. The results show that *Ulva* are mainly composed of calcium at a concentration of 47653.960 ppm and potassium at a concentration of 45509.600 ppm. Minor elements were also detected, such as magnesium (8077.350 ppm), sulfur (4977.710 ppm), phosphorus (3055.046 ppm), and iron (2493.788 ppm). Other elements such as mercury, lead, and cadmium were not detected in the *Ulva sp.* samples, their concentrations being below the detection limit. A study on the characterization of macroalgae of the type *Ulva pilifera* gave a partially comparable elemental profile, with the presence in the *Ulva* thalli of 14 elements (Al, Ba, Br, Ca, Cl, Fe, I, K, Mg, Mn, Na, P, S, and Si). The latter showed that the major element was calcium at a concentration of 16.3%, and the minor elements were sulfur at 1.86%, silicon at 1.67%, and magnesium at 0.999% (Czerwik-Marcinkowska et al., 2020). Another recent study on the characterization of *Ulva sp.* revealed that the major element was sodium with a concentration of 73.80 ± 0.45 mg/g (Mouga et al., 2025).

Table I: Mineral composition of the macroalga *Ulva sp.*

Elements	Values in ppm (mg/Kg)
Mo	0.112
Pb	< 0.001
Se	0.174
As	25.86
Hg	< 0.001
Zn	20.378
Cu	1.145
Ni	0.192
Co	0.402
Fe	2493.788
Mn	229.17
Cr	0.795
Ca	47653.96
K	45509.6
S	4977.71
Cd	< 0.001
Mg	8077.35
P	3055.046

3.1. Physical and chemical Characterization of *Ulva*

The values of the physicochemical parameters such as moisture content, ash content, total organic carbon, and lower heating value are presented in Table II. Each experiment was repeated twice to evaluate the standard deviation.

Table II: Physical and chemical parameters of the briquettes

Physical and chemical Parameters	BAL50	BAL40	BAL30	BAL20	CHARCOAL
Moisture Content (%)	6.64±0.026	6.76±0.032	6.84±0.027	6.93±0.031	5.14±0.019
TOC (%)	15.71±0.019	20.11±0.025	21.96±0.016	24.33±0.023	20.61±0.024
Ash Content (%)	49.75±0.041	47.3±0.035	44.94±0.037	39.38±0.029	17.54±0.023
LHV (kcal/kg)	1289±0.024	1338±0.029	1365±0.031	1778±0.028	2939±0.032

3.2. Ash and Moisture Content

Ash content represents the amount of inorganic elements and other minerals composing the biomass that do not burn, thus leaving residues after combustion (Imaniraguha et al., 2025). Briquettes with 50% binder are those with the highest ash content (49.75%), while the BAL20 sample has the lowest ash content among the briquettes (39.38%), but this is still much higher than that of charcoal (17.54%). This difference is mainly explained by the mineral nature of the binder, rich in inorganic elements that directly contribute to ash formation. Additionally, the presence of exogenous materials such as gastropods or sand in the *Ulva sp.* biomass can also increase this content (Bird et al., 2011). The values obtained here are within

the range reported by Olufunke O. Oyebamiji et al., which varied from 16.70% (groundnut shell) to 79.25% (maize straw) (Oyebamiji et al., 2025). A study has also shown that the presence of compounds like sodium, potassium, phosphorus, and chlorine in macroalgae contributes to the increase in ash content (Bilodeau et al., 2022).

Regarding moisture, the briquettes present values within a narrow range, between 6.64% and 6.93%. These contents are slightly higher than that of charcoal (5.14%) and that obtained by Georges et al. for algae-based briquettes (4.83%). This higher moisture can be attributed to the hygroscopic nature of the binder which, suspended in water, swells and retains a significant amount of water to form an interstitial layer (Lomunyak et al., 2024). According to Nakimuli et al., an optimal moisture content improves the density, durability, and compressive strength of briquettes (Nakato et al., 2025). Figure 7 presents a comparison of ash and moisture contents for the different samples.

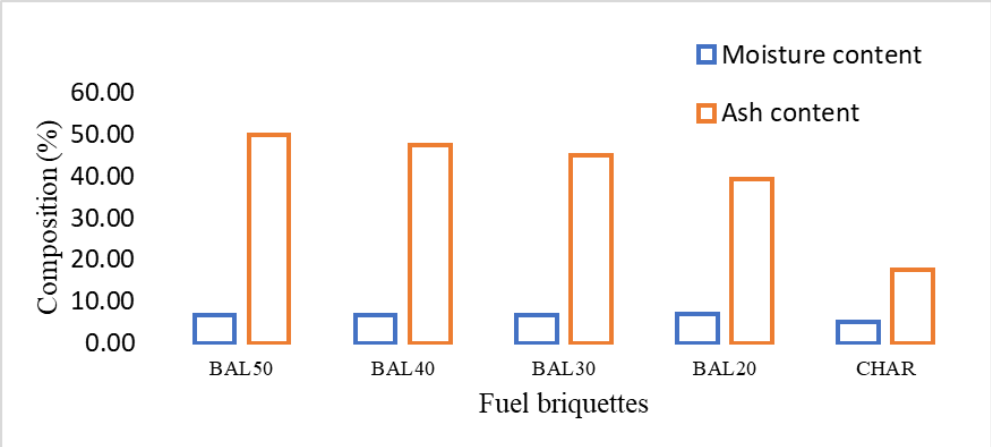

Figure 7: Influence of binder percentage on moisture content and ash content

3.4. Total Organic Carbon (TOC)

Total organic carbon includes all forms of organic carbon, whether dissolved, volatile, or solid. It differs from fixed carbon, which corresponds to the carbon fraction remaining after removal of moisture, volatile matter, and ash. Among all the samples analyzed, the TOC content varies from 15.71% to 24.33%. It decreases with the progressive addition of binder from 20 to 50%. The binder used is a mineral material; its incorporation at high levels contributes to the decrease in organic carbon content. BAL20 type briquettes have a TOC content of 24.33%, higher than BAL50, BAL40, and BAL30. It has been reported in the literature that the biomass of green algae of the type *Ulva sp.* is very rich in organic compounds (Toro-Mellado et al., 2025). This is why Dogmaz and Cavas used biomass from *Ulva lactuca* proliferations to produce biohydrogen via silver nanoparticles

(Dogmaz & Cavas, 2023). Figure 8 shows the total organic carbon content of the different briquettes.

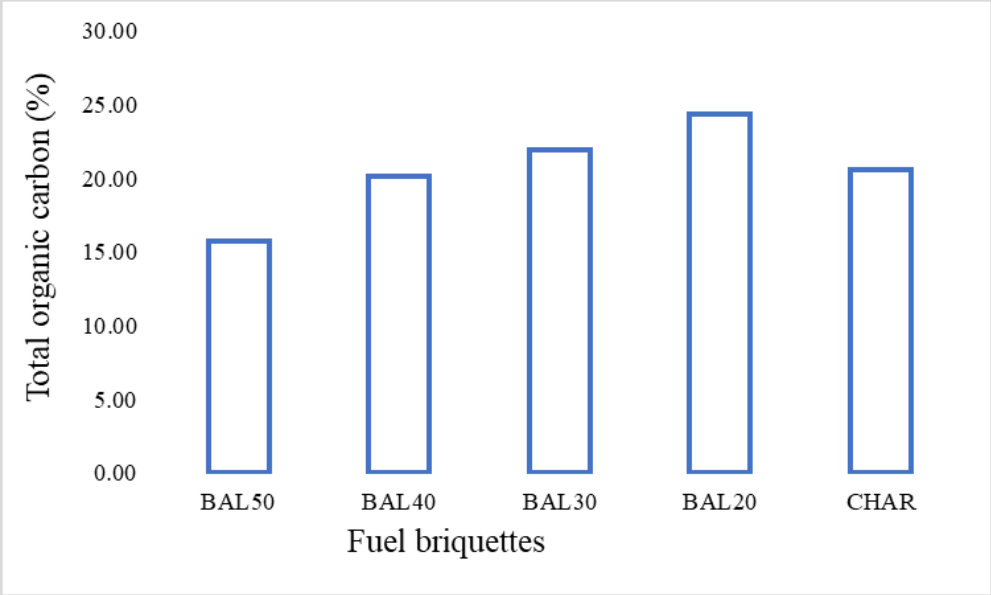

Figure 8: Influence of binder percentage on TOC

3.3. Lower Heating Value (LHV)

The results obtained show that the LHV of charcoal (2939 kcal/kg) is higher than that of the designed fuel briquettes. This high value is explained by the presence of lignin, whose decomposition generates a high rate of fixed carbon. However, only the BAL20 type briquettes have an LHV relatively close to that of coal, with about 1778 kcal/kg (Note: The abstract mentions 2254 kcal/kg for BAL20, but Table II shows 1778. We'll use the table value here for consistency, but this discrepancy should be noted). While the other types of briquettes, namely BAL50, BAL40, BAL30, give low LHV values. This decrease in calorific value can be explained by the presence of the binder in the samples and also the rather low organic carbon content. Calcium silicate impoverishes the LHV of combustible briquettes due to the presence of minerals within it. The value obtained for BAL20 is lower than that of Brice et al., which is 10 MJ/kg (approx. 2388 kcal/kg). This observed difference is explained by the fact that their briquettes were designed using wood, whose lignin and cellulose contents are 26.6% and 50.4%, respectively (Martial et al., 2025). Figure 9 illustrates the LHV of the different fuels.

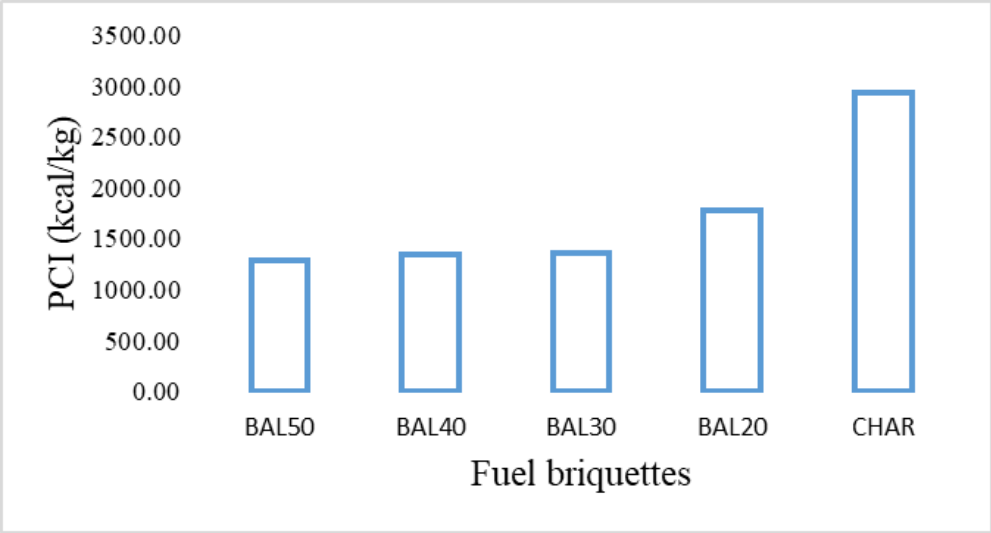

Figure 9: Influence of binder percentage on LHV

3.4. Analysis of Variance (ANOVA)

The analysis of variance performed on the calorific value as a function of moisture content and total organic carbon shows that the variability of the lower heating value (LHV) can be partially explained by the ash content (ASH). The results indicate that the effect of ash content (ASH) is highly significant ($p = 0.0307 < 5\%$), indicating a clear influence of ash content on LHV. In contrast, moisture content (H) ($p = 0.4547 > 5\%$) and total organic carbon (TOC) ($p = 0.4432 > 5\%$) did not show significant effects at the significance level $\alpha = 0.05$, suggesting that moisture content and total organic carbon do not exert a statistically detectable influence on the lower heating value. Similar results were reported by Huihui Liu et al. in the study of hydrothermal carbonization of natural microalgae with high ash content (Liu et al., 2019). The different effects of ash content, total organic carbon, and moisture content on the lower heating value are illustrated in Figure 10.

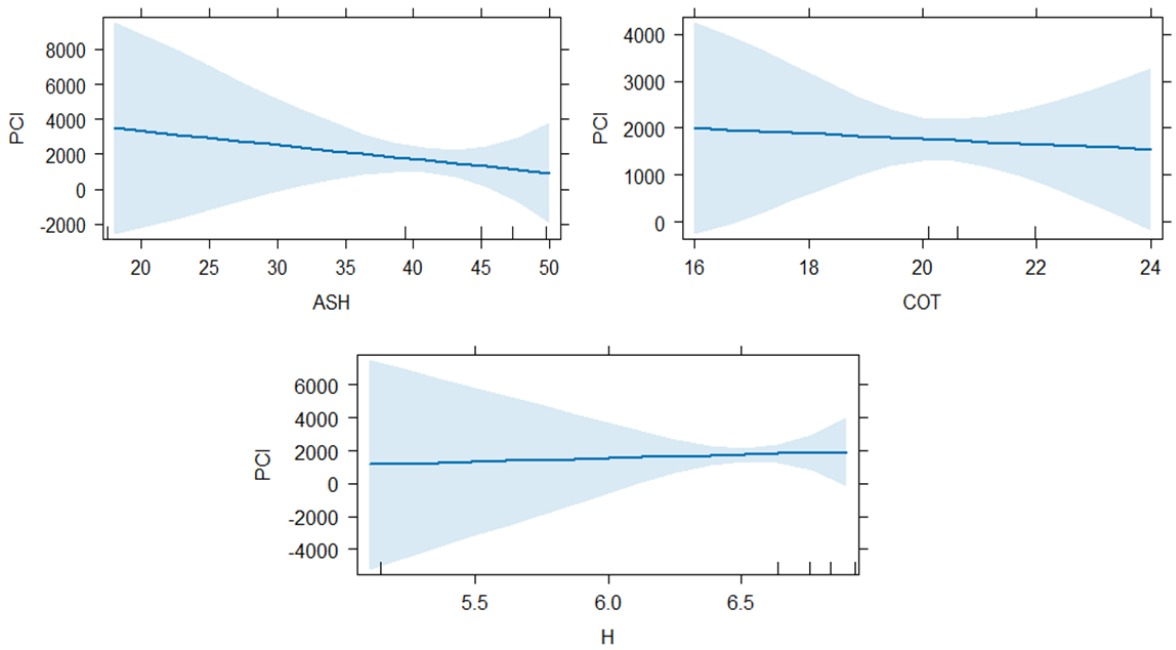

Figure 10: Effects of ash content, total organic carbon, and moisture on lower heating value

3.5. Shatter Resistance

It represents an indicator of briquette rigidity. Evaluating this parameter provides information on the behavior of briquettes during handling, transport, and storage. According to Table III, BAL50 presents the highest durability (84%), a value clearly superior to that of the other samples. These results are justified by a high presence of calcium silicate. This value is lower than that obtained by Gordian Akam et al., which is 125% for the briquette from cocoa waste (Akam et al., 2024). Nonsawang et al. reported that shatter resistance is a function of binder content. Increasing binder content leads to high shatter resistance (Nonsawang et al., 2024). According to Mitchual et al., briquettes with shatter resistance greater than 80% are very durable (Mitchual et al., 2013).

Table III: Influence of calcium silicate percentage on shatter resistance

Briquettes	BAL50	BAL40	BAL30	BAL20
Mechanical Durability	0.84	0.82	0.81	0.79

3.6. Combustion Test

Figure 11 shows the evolution of the water temperature, measured every 5 minutes during heating with the different types of briquettes. The temperature at which the water began to boil (> 90°C) served as a reference indicator. The BAL20 type briquettes reach 101.7°C after 25 minutes, which is why their combustion is slower and sustained. For BAL30, a progressive

temperature rise is observed up to 84.7°C at about 25 minutes with a somewhat stable thermal plateau. The BAL40 and BAL50 type briquettes reach their respective peaks at 69.6°C after 25 min and 77.6°C after 30 min with less efficient combustion. This poor combustion of BAL40 and BAL50 is probably due to the presence of very high ash content, moisture, and volatile organic matter. According to Gang Li et al., several factors can affect the combustion rate, and in their study, it was hypothesized that the higher ash content (54.3 ± 0.9%) of the fuel was the main reason for the lower combustion rate (G. Li et al., 2022). Another study on sawdust briquettes showed that energy efficiency decreased with increasing moisture, which can reduce the combustion rate (Mkini & Bakari, 2018).

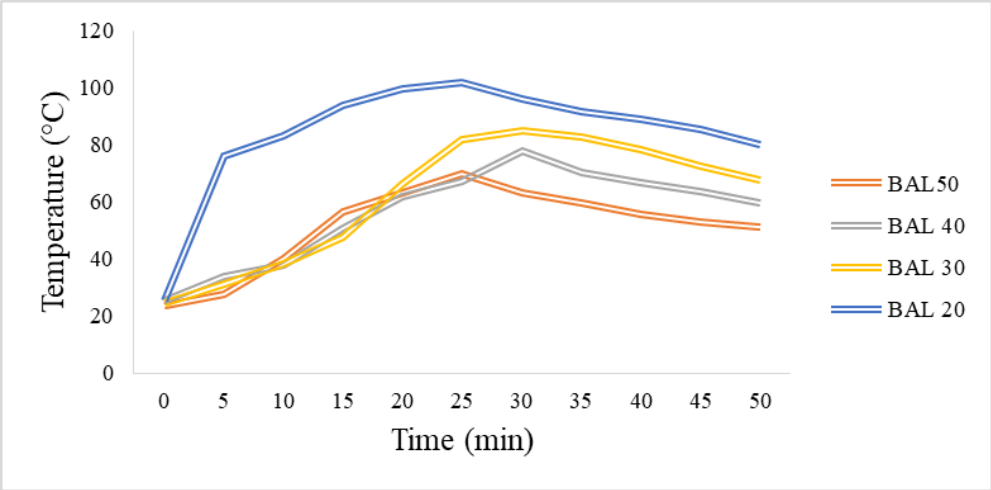

Figure 11: Evolution of water boiling temperature over time

Conclusion

This study aimed to valorize *Ulva sp.* waste from the SENELEC C3 power plant into combustible briquettes, an alternative to conventional coal. In this regard, it demonstrates the technical feasibility of the energy valorization of *Ulva sp.* macroalgae, widely available in Senegal, through the manufacture of combustible briquettes. The results indicate that the mineral binder content (calcium silicate) significantly influences the combustible and mechanical properties of the briquettes. Among the tested formulations, briquettes with 20% binder (BAL20) show the most promising performance, with a lower heating value (LHV) of 1778 kcal/kg and a prolonged combustion duration (85 minutes), although they remain inferior to conventional charcoal (LHV = 2939 kcal/kg).

Statistical analysis (ANOVA) confirmed that ash content is the predominant factor affecting LHV, with a significant effect ($p = 0.0307$), unlike moisture or total organic carbon. Furthermore, the mechanical

resistance of the briquettes increases with the proportion of binder, reaching an optimal durability of 84% for BAL50.

However, the high ash content of the briquettes, particularly for BAL20 (39.38%), raises challenges for large-scale use, particularly in terms of residue management and impact on combustion systems. Further studies are needed to characterize the ash composition, optimize production processes, and evaluate the environmental and economic sustainability of this emerging sector.

Despite these limitations, this study opens promising perspectives for the sustainable valorization of algal biomasses, contributing to the energy transition and reducing pressure on forest resources.

Conflict of Interest: The authors reported no conflict of interest.

Data Availability: All data are included in the content of the paper.

Funding Statement: The authors did not obtain any funding for this research.

References:

1. Ahmed, M. S., Lebrini, M., Pellé, J., Rioual, S., Amintas, O., Boulanger, C., Lescop, B., & Roos, C. (2024). Study of atmospheric corrosion of zinc in a tropical marine environment rich in H2S, resulting from the decomposition of Sargassum algae. *Materials and Corrosion*, *75*(9), 1133–1141. https://doi.org/10.1002/MACO.202414292.
2. Akam, N. G., Diboma, B. S., Mfomo, J. Z., Ndiwe, B., Bôt, B. V., & Biwolé, A. B. (2024). Physicochemical characterization of briquette fuel produced from cocoa pod husk case of Cameroon. *Energy Reports*, *11*(September 2023), 1580–1589. https://doi.org/10.1016/j.egyr.2024.01.029.
3. Amrullah, A., Farobie, O., Bayu, A., Syaftika, N., Hartulistiyoso, E., Moheimani, N. R., Karnjanakom, S., & Matsumura, Y. (2022). Slow Pyrolysis of Ulva lactuca (Chlorophyta) for Sustainable Production of Bio-Oil and Biochar. *Sustainability (Switzerland)*, *14*(6), 1–14. https://doi.org/10.3390/su14063233.
4. B-m, S., B-m, L., Acevedo, F., Ernstgård, L., Johanson, G., Larsson, K., Palmberg, L., Sundblad, B., Larsson, B., Acevedo, F., & Ernstgård, L. (2004). *Acute respiratory effects of exposure to ammonia on healthy persons*. *30*(4), 313–321.
5. BA, K., DIOP, E. H. M., TOURE, A. O., & SAMBE, F. M. (2022). Optimization of cristal violet adsorption by calcium silicate waste

material. *Scientific African*, *18*, 01417. https://doi.org/10.1016/j.sciaf.2022.e01417

6. Baghel, R. S., Suthar, P., Gajaria, T. K., Bhattacharya, S., Anil, A., & Reddy, C. R. K. (2020). Seaweed biore fi nery: A sustainable process for valorising the biomass of brown seaweed. *Journal of Cleaner Production*, *263*, 121359. https://doi.org/10.1016/j.jclepro.2020.121359
7. Bilodeau, M., Barnabé, S., Riverin, L., & Fequet, K. (2022). *Potentiel d'intégration des algues marines de la basse-côte-nord dans le mix énergétique québécois*. 43–47.
8. Bird, M. I., Wurster, C. M., de Paula Silva, P. H., Bass, A. M., & de Nys, R. (2011). Algal biochar - production and properties. *Bioresource Technology*, *102*(2), 1886–1891. https://doi.org/10.1016/j.biortech.2010.07.106
9. Czerwik-Marcinkowska, J., Piwowarczyk, R., Uher, B., Tomal, E., & Wojciechowska, A. (2020). X-ray Fluorescence Techniques in Determining the Habitat Preferences of Species—Ulva pilifera (Ulvales, Chlorophyta) from Montenegro Case Study. *Molecules*, *25*(21). https://doi.org/10.3390/molecules25215022
10. Dogmaz, S., & Cavas, L. (2023). Biohydrogen production via green silver nanoparticles synthesized through biomass of Ulva lactuca bloom. *Bioresource Technology*, *379*(April), 129028. https://doi.org/10.1016/j.biortech.2023.129028
11. François, M., Lin, K., Hussain, J., & Mdlovu, N. V. (2025). Enhancement of biomass energy: thermal conversion , biogas yield , and machine learning insights. *Journal of the Energy Institute*, *121*(May), 102131. https://doi.org/10.1016/j.joei.2025.102131
12. Imaniraguha, J., Mushimiyimana, T., Lucas, C., & Condo, A. (2025). Production and characterization of briquettes from Panicum maximum Jacq . (guinea grass) and cassava peel waste. *Energy Reports*, *14*(June), 1043–1050. https://doi.org/10.1016/j.egyr.2025.07.033
13. Jabeen, F., Zil-E-Aimen, N., Ahmad, R., Mir, S., Awwad, N. S., & Ibrahium, H. A. (2025). Carrageenan: structure, properties and applications with special emphasis on food science. *RSC Advances*, *15*(27), 22035–22062. https://doi.org/10.1039/d5ra03296b
14. Jo, J. Y., Kwon, Y. S., Lee, J. W., Park, J. S., Rho, B. H., & Choi, W. Il. (2013). Acute respiratory distress due to methane

inhalation. *Tuberculosis and Respiratory Diseases*, *74*(3), 120–123. https://doi.org/10.4046/trd.2013.74.3.120

15. Kim, G., Hwan, Y., Kim, I., & Han, J. (2019). Science of the Total Environment Co-production of biodiesel and alginate from Laminaria japonica. *Science of the Total Environment*, *673*, 750–755. https://doi.org/10.1016/j.scitotenv.2019.04.049
16. Lars Ole Goffeng , Åse Dalseth Austigard, Kristin H Svendsen, Øivind Skare, Elin Einarsdottir, Lene Madsø, K. K. H. (2023). *Étude transversale de la fonction neuropsychologique sensorimotrice chez les travailleurs des stations d'épuration et des réseaux d'assainissement exposés au sulfure d'hydrogène lors de la manipulation des eaux usées - PubMed*. https://pubmed.ncbi.nlm.nih.gov/37742044/
17. Li, C., Liang, Y., Miao, Q., Ji, X., Duan, P., & Quan, D. (2024). The Influence of Microalgae Fertilizer on Soil Water Conservation and Soil Improvement: Yield and Quality of Potted Tomatoes. *Agronomy*, *14*(9). https://doi.org/10.3390/agronomy14092102
18. Li, G., Hao, Y., Yang, T., Wu, J., Xu, F., Li, L., Wang, B., Li, M., Zhao, N., Wang, N., Liu, C., Huang, Z., Zhou, Y., & Zhao, Y. (2022). Air pollutant emissions from sludge-bituminous briquettes as a potential household energy source. *Case Studies in Thermal Engineering*, *37*(June), 102251. https://doi.org/10.1016/j.csite.2022.102251
19. Liu, H., Chen, Y., Yang, H., Gentili, F. G., Söderlind, U., Wang, X., Zhang, W., & Chen, H. (2019). Hydrothermal carbonization of natural microalgae containing a high ash content. *Fuel*, *249*(March), 441–448. https://doi.org/10.1016/j.fuel.2019.03.004
20. Lomunyak, G., Osodo, B., Njoka, F., & Kombe, E. (2024). Heliyon Characterization, optimization and emission analysis of manually-made charcoal dust briquettes with starch , paper and algae binders. *Heliyon*, *10*(24), e40991. https://doi.org/10.1016/j.heliyon.2024.e40991
21. Martial, B., Lemaire, R., & Nikiema, J. (2025). Industrial Crops & Products Insight into the production factors influencing the physicochemical properties of densified briquettes comprising wood shavings and rice husk. *Industrial Crops & Products*, *223*(November 2024), 120134. https://doi.org/10.1016/j.indcrop.2024.120134

22. Mitchual, S. J., Frimpong-mensah, K., & Darkwa, N. A. (2013). *Effect of species , particle size and compacting pressure on relaxed density and compressive strength of fuel briquettes*. 2–7.
23. Mkini, R. I., & Bakari, Z. (2018). Effect of Moisture Content on Combustion and Friability Characteristics of Biomass Waste Briquettes Made By Small Scale Producers in Tanzania. *International Journal of Engineering Research and Reviews*, *3*(1), 66–72. www.researchpublish.com
24. Mouga, T., Almeida, M. M., Pitacas, F. I., Rodrigues, A. M., Vitória, C., & Anjos, O. (2025). Elemental and Nutritional Characterisation with Vibrational Spectroscopy Analysis of Ulva sp., Gracilaria multipartita, and Sargassum muticum. *Applied Sciences (Switzerland)*, *15*(8), 1–24. https://doi.org/10.3390/app15084212
25. Nakato, C., Kaggwa, F., Greef, J. De, Kilama, D., Blondeau, J., & Kawuma, S. (2025). Green Energy and Resources Review of machine learning applications for predicting the quality of biomass briquettes for sustainable and low-carbon energy solutions. *Green Energy and Resources*, *3*(3), 100130. https://doi.org/10.1016/j.gerr.2025.100130
26. Nations, F. and A. O. of the U. (2024). The State of World Fisheries and Aquaculture. In *Nature and Resources* (Vol. 35, Issue 3).
27. Nonsawang, S., Juntahum, S., Sanchumpu, P., & Suaili, W. (2024). *Unlocking renewable fuel: Charcoal briquettes production from agro-industrial waste with cassava industrial binders*. *12*(November), 4966–4982.
28. Nzihou, A., Ifunanya, G., & Gonz, M. (2024). *A review on biochar briquetting: Common practices and recommendations to enhance mechanical properties and environmental performances*. *469*(March). https://doi.org/10.1016/j.jclepro.2024.143193
29. Oyebamiji, O. O., Olaleru, A. S., Oyeleke, R. B., & Ofodile, L. N. (2025). Evaluation and characterization of biochar and briquettes from agricultural wastes for sustainable energy production. *Waste Management Bulletin*, *3*(3), 100198. https://doi.org/10.1016/j.wmb.2025.100198
30. Rath, D. P., Mahapatro, A., & Pattanayak, B. (2024). Materials Today: Proceedings Briquette production and performance evaluation from coal and agricultural waste. *Materials Today: Proceedings*, *October 2023*. https://doi.org/10.1016/j.matpr.2023.12.019
31. Sundaram, T., Kamalesh, R., Saravanan, A., Yaashikaa, P. R., Vickram, A. S., Teena, R. A., & Thiruvengadam, S. (2025).

International Journal of Biological Macromolecules Harnessing algal biomass for renewable energy and biofuel production: Current strategies and future insights ☆. *International Journal of Biological Macromolecules*, *319*(P2), 145487. https://doi.org/10.1016/j.ijbiomac.2025.145487

32. Toro-Mellado, F., Piña, F., Baltrusch, K. L., Inoubli, S., Flórez-Fernández, N., Torres, M. D., Contreras-Porcia, L., & Domínguez, H. (2025). Potential applications of Ulva spp. *Food Bioscience*, *71*(July). https://doi.org/10.1016/j.fbio.2025.107256
33. Wal, H. Van Der, Sperber, B. L. H. M., Houweling-tan, B., Bakker, R. R. C., Brandenburg, W., & López-contreras, A. M. (2013). Bioresource Technology Production of acetone , butanol , and ethanol from biomass of the green seaweed Ulva lactuca. *Bioresource Technology*, *128*, 431–437. https://doi.org/10.1016/j.biortech.2012.10.094
34. Yaman, S., & Kucukbayrak, S. (2013). Production of biobriquettes from carbonized brown seaweed. *Fuel Processing Technology*, *106*, 33–40. https://doi.org/10.1016/j.fuproc.2012.06.014